

Electronic Supplementary Information (ESI)

Promoting Photothermal Antibacterial Activity through Excited-State

Intramolecular Proton Transfer process

Wanni Yao, ‡^a Tian Deng, ‡^b Arui Huang, ‡^a Yufeng Zhang, *^b Qianqian Li, *^a Zhen Li*^{ac}

^a Hubei Key Lab on Organic and Polymeric Opto-Electronic Materials, TaiKang Center for Life and Medical Sciences, Sauvage Center for Molecular Sciences, Department of Chemistry, Wuhan University, Wuhan, 430072 China

^b State Key Laboratory Breeding Base of Basic Science of Stomatology (Hubei-MOST), Key Laboratory of Oral Biomedicine Ministry of Education, School and Hospital of Stomatology, Wuhan University, Wuhan, 430079 P. R. China

^c Institute of Molecular Aggregation Science, Tianjin University, Tianjin, 300072 China

Materials and methods

General methods

¹H NMR and ¹³C NMR spectra were recorded on a 400 MHz Bruker Ascend spectrometer using methanol-*d*₄ as solvent. UV-vis spectra were performed on a Shimadzu UV-2550 and an Ocean Optics QE65 Pro spectrometer. The single-crystal X-ray diffraction data was collected in a Bruker Smart Apex CCD diffractometer. High resolution mass spectrometry (HRMS) was measured using a Bruker Ultimate3000 & Compact mass spectrophotometer. High performance liquid chromatography (HPLC) was conducted on LaboACE LC-5060 PlusII. Mechanical tests were carried out by a universal tensile-compressive tester (CMT 6503, Shenzhen SANS Test Machine, Shenzhen, China). Photoluminescence spectra were recorded by a Hitachi F-4600 fluorescence spectrophotometer. UV Light (365 nm) was obtained from an LED lamp irradiator (CCS, HLV-24GR-3W).

Synthesis of DOA

2,4-Dihydroxybenzaldehyde (1.00 g, 7.13 mmol) and 4-aminophenol (0.76 g, 7.13 mmol) were dissolved in ethanol (30 mL). The reaction mixture stirred at 70 °C for 3 h. After removal of the solvent under reduced pressure, the crude product was recrystallized to yield brown crystals (1.10 g, 63%). ¹H NMR (400 MHz, methanol-*d*₄) δ (ppm): 8.61 (s, 1H, ArCH=N), 7.28 (d, *J* = 8.5 Hz, 1H, ArH), 7.26-7.18 (m, 2H, ArH), 6.89-6.81 (m, 2H, ArH), 6.35 (dd, *J* = 8.5, 2.2 Hz, 1H, ArH), 6.27 (d, *J* = 2.3 Hz, 1H, ArH). ¹³C NMR (100 MHz, methanol-*d*₄) δ (ppm): 163.28, 160.21, 156.69, 139.58, 134.39, 116.37, 112.61, 108.04, 102.83. HRMS (ESI, *m/z*): [M+H]⁺ calcd for C₁₃H₁₁NO₃: 230.0805, found 230.0812.

Sample preparation

Firstly, polymer PVA (7.5 g) was dissolved in deionized water (50 mL), and stirred for 1.5 h at 90 °C to obtain a homogeneous 15 wt% PVA solution. The aqueous dispersion of DOA was sonicated for 40 minutes, then added dropwise into the PVA solution with the concentration of 1 wt%. Afterward, the mixed solution was vigorously stirred for 0.5 h, and then poured into a PTFE mold. Finally, the mold was placed at -20 °C for 24 hours. After the freezing process, it was allowed to thaw at 23 °C for 24 h. Two freezing-thawing cycles were used for the DPVA hydrogel preparation.

Mechanical test

All mechanical tests were performed at room temperature using a universal tensile-compressive tester (CMT 6503, Shenzhen SANS Test Machine, Shenzhen, China) equipped with a 200 N load cell. For tension, the hydrogel with square shape (length of 50 mm, width of 10 mm, and thickness of 1 mm) was measured at a rate of 50 mm min⁻¹. For compression, the hydrogel with cylindrical shape (height of 10 mm and diameter of 15 mm) was measured at a rate of 5 mm min⁻¹. The tensile stress (σ) was defined as the loading force (F) divided by the cross-sectional area (A_0) of the original sample ($\sigma = F/A_0$). The tensile strain (ε) was defined as the deformed length divided by the original length ($\varepsilon = (L - L_0)/L_0$). Toughness (T) was obtained by integrating the area underneath the stress-strain curve by following equation:

$$T = \int_{\varepsilon_0}^{\varepsilon_f} \sigma(\varepsilon) d\varepsilon$$

where ε_f and ε_0 were the initial strain and fracture strain, respectively. The elastic modulus (E) was calculated according to the initial linear slope of the stress-strain curve (0.1-2% strain).

Evaluation of photothermal effect

A 365 nm LED lamp (average power density: 210 mW cm⁻²) was focused on the DPVA hydrogel (0.8 cm × 0.8 cm × 1.0 mm) for 100 s. The infrared thermal images were taken every 10 seconds with a fluke tis60+ thermal imaging camera. The experiments were repeated for five times to get an average value. The real-time temperature of PVA hydrogel was also measured as reference.

Bacteria culture

Staphylococcus aureus, *Methicillin-resistant Staphylococcus aureus*, *Escherichia coli*, and *Enteroinvasive E. coli* were used in experiments and represented Gram-positive bacteria and Gram-negative bacteria respectively. Before antibacterial experiments, *S. aureus* and *MRSA* was routinely cultured in BHI medium at 37 °C. *E. coli* and *EIEC* routinely grew in LB medium at 37 °C. Bacteria used in all experiments were in the mid-exponential growth phase.

Observation of *in vitro* colony-forming units

Bacterial suspensions were vortexed and measured at OD 600 nm using Spectramax i3x (Molecular Devices, USA). Then, the suspensions were diluted to 1 × 10⁹ CFU · mL⁻¹, and 10 μL of them were dropped into the wells of 24-well plates. Afterwards, the hydrogels were placed on the suspension drop respectively. Each sample in UV exposure group was then irradiated with 365 nm LED lamp for 100 s. Notably, the plate of DPVA (ice) group was irradiated on an ice bath. Then all the samples were added into PBS (990 μL) and washed carefully. Next, the suspensions in the wells were diluted 10-fold, and 10 μL of them was spread on solid medium. The plates were incubated for 24 h before the number of bacterial colonies was counted.

Bacterial live/dead staining

The suspension of bacteria was diluted into 1 × 10⁹ CFU/mL and 10 μL of them were dropped into the wells of 24-well plates. Afterwards, the hydrogels were placed on the suspension drop respectively. Each sample in UV exposure group was then irradiated with 365 nm LED lamp for 100 s. Notably, the plate of DPVA (ice) was irradiated with ice bath. Then, the hydrogels were removed and the samples were incubated in the dark for 1.5 h using a Live-Dead Stain kit (Beyotime, China). Finally, we utilized Olympus D71 fluorescence microscope to take photos and analyzed the red and green fluorescence by Image J software.

Scanning electron microscope observation of the bacteria

Bacterial morphology was investigated *via* SEM. Briefly, bacteria were incubated into the mid-exponential growth phase and bacterial suspensions were dropped to 24-well plates. The liquid was covered by DPVA hydrogel or PVA hydrogel respectively, under UV irradiation with 365 nm LED lamp for 100 s. Besides, the plate of DPVA (ice) was irradiated with ice bath. The culture medium was removed and the bacteria were fixed by 2.5% glutaraldehyde overnight. Before being dehydrated using 50%, 75%, 90% and 100% ethanol, the samples were washed twice with deionized water. Finally, the samples were dried by the critical point drying method, coated with platinum, and observed by SEM.

Growth curves measurements

The suspension of bacteria was diluted into 1×10^9 CFU/mL, and 10 μ L of them were dropped into the wells of 24-well plates. Afterwards, the hydrogels were placed on the suspension drop respectively. Each sample in UV exposure group was then irradiated with 365 nm LED lamp for 100 s. Notably, the plate of DPVA (ice) was irradiated with ice bath. Next, 10 μ L of each sample suspension was added with 990 μ L LB or BHI medium and 200 μ L of them were transferred to a 96-well plate, and incubated at 37 °C. OD 600 values were measured every 2 h for 12 h.

Biocompatibility Evaluation *in vitro*

L929 cells were cultured in 96-well plate with Dulbecco's modified Eagle's medium (Gibco, USA) containing 10% fetal bovine serum (Gibco, USA) and 1% penicillin-streptomycin solution (Gibco). The extraction solution of hydrogels was added into subject groups, while PBS was dropped into the control group. Then the cytotoxicity of the materials was evaluated using CCK8 reagent (Vazyme, China). After coculture for 24 h and 48 h, the old medium was replaced with CCK8 solution for 2 h of incubation at 37°C. The absorbance of each well was measured at 490 nm.

Phototoxicity test *in vitro*

RAW264.7 cells were cultured in 96-well plate with high- glucose Dulbecco's modified Eagle's medium (Gibco, USA) containing 10% fetal bovine serum (Gibco, USA) and 1% penicillin-streptomycin solution (Gibco). Then the DPVA or PVA hydrogels were placed onto the wells. There was nothing covered on the wells in the control group. Next, the wells were irradiated by 365 nm LED lamp for 100 s and incubated at 37 °C for 12 h. The cells were taken photos by microscopy, and old medium was replaced with CCK8 solution for 2 h of incubation at 37 °C. The absorbance of each well was measured at 490 nm.

Observation of photothermal effect *in vivo*

KM mice (8-week-old, female) were used in this study. The animal study protocol was approved by the Committee for Animal Research of Wuhan University. Briefly, the back of mice was carefully shaved by electronic trimmers and 20 μ L of PBS solution was dripped onto the backs of mice. Then the backs of mice were covered by DPVA or PVA hydrogels. For the PBS group, there was nothing covered on the back of mice. Then the mice were exposed to 365 nm LED lamp for 100 s and the local temperature together with thermal images were recorded by FLIR.

Infection wounds modeling

Before experiments, the bacteria were incubated into the mid-exponential growth phase. Then the hair on the back was shaved carefully by shaved electronic trimmers and hair removal cream (Veet, France), and both left and right sites were chosen to form infection wounds. Afterwards, full thickness wounds were performed by 8

mm biopsy punch. Then the wounds were applied with 20 μ L bacterial suspensions and covered by PVA or DPVA hydrogels respectively. The wounds on the left were exposed to the 365 nm LED lamp for 100 s, while the right ones were treated as control without UV irradiation. After UV treatment, the hydrogels were removed and the wounds were covered by Tegaderm (3M, USA). The skin lesions were taken photos on the 7th and 20th day and the size of them were measured by Image J.

Evaluation of *in vivo* antibacterial effect

As mentioned above, after the lesion sizes of subcutaneous abscess were measured, the mice were sacrificed 7 days after bacterial infection and the wounds were harvested by sterilized scissors and immersed in PBS solutions. Then the tissues were fully ground and the grinding fluid was collected respectively. The samples were diluted 100, 500 and 2000 times, and 10 μ L suspension was spread on solid medium. The solid medium plates were incubated at 37 °C for 24 h and the colony forming units were counted.

Histological staining

The mice were sacrificed on the 7th and 20th day. Before being fixed in 4% paraformaldehyde solution overnight, the skin lesions were harvested by sterilized scissors. Then the specimens were dehydrated with sequential treatment with 50, 70, 80, 90, 95 and 100% ethanol for 30 mins and were immersed in *n*-butyl alcohol overnight. Next, the samples were embedded in paraffin. Hematoxylin and eosin (H&E) staining was performed to evaluate the bacterial infection and inflammation, while the Massion staining was utilized to observe the generation of vessels and collagen.

Hemolysis test

Fresh mouse blood was used to perform hemolysis tests. Briefly, the blood was centrifuged (1500 rpm, 5 min) several times, until the supernatant was colorless and transparent. Then the supernatant was discarded, and the erythrocytes were collected and diluted into 8 mL by PBS. Next, the erythrocytes suspensions were added with DPVA or PVA hydrogel extract. The suspension of negative group was dropped with PBS, while that of positive group was added with erythrocytes lysis buffer (Beyotime, China). After being incubated at 4 °C for 4 h, the samples were centrifuged (1500 rpm, 10 min) and taken photos. 100 μ L supernatants were transferred to a 96-well plate and the intensity of OD. 570 nm was recorded.

Results and discussions

Table S1 Quantum Yield of OA and DOA.

Sample	Quantum Yield (Φ , %)		
	doped in PVA ^a	in hexane solution ^b	in ethanol solution ^b
OA	6.21	3.40	1.08
DOA	1.30	3.61	1.17

^a Doping ratio: 1wt%, ^b concentration: 2×10^{-5} mol L⁻¹

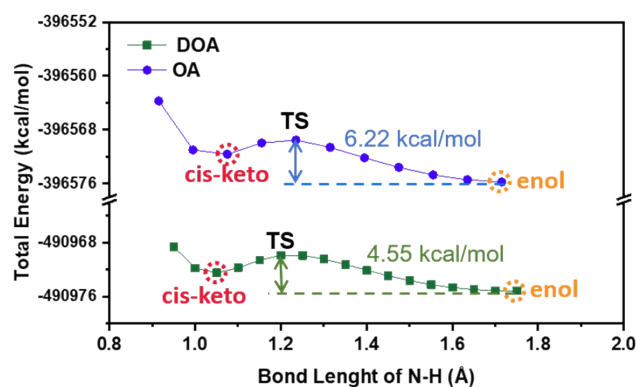


Figure S1. Potential energy surface of OA and DOA from enol to *cis*-keto form. Note: The transformation from enol to *cis*-keto can be considered as the break of O-H bond and the closeness of N-H bond. The potential energy surface (PES) of the transformation process for OA and DOA indicates the existence of one transition state (TS). Then the TS was optimized and checked by calculating IRC to give the energy barrier of the reaction.

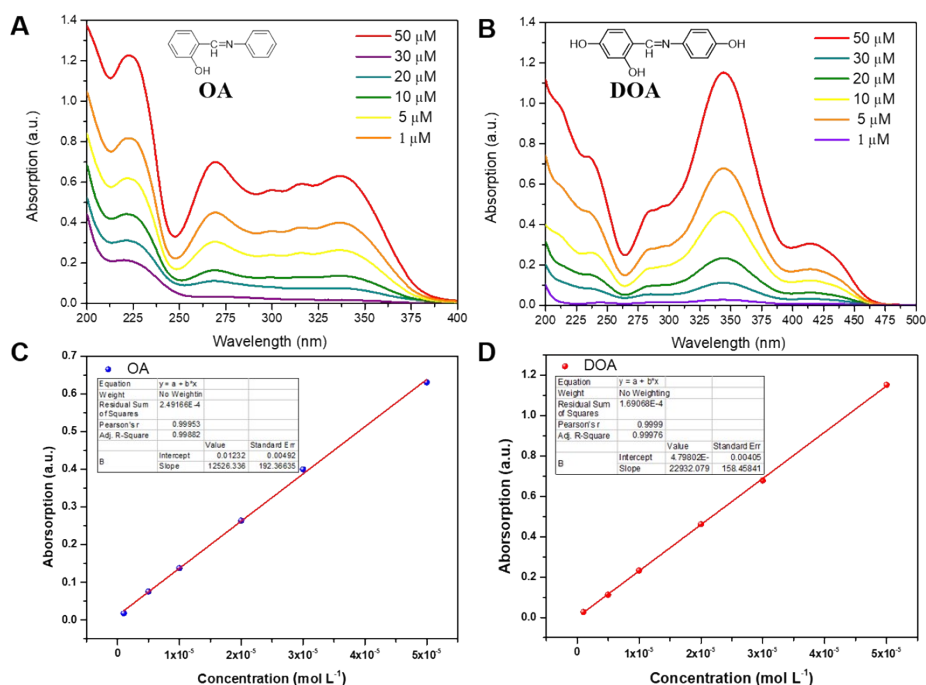


Figure S2. The UV absorption spectra of OA (A) and DOA (B) in methanol solution with different concentrations. The molar extinction coefficient fitting curves of OA (C) (336 nm) and DOA (D) (344 nm).

Table S2 Detailed information of photothermal hydrogels.

Sample	Photothermal agent	Excitation light source	$\Delta T / T_{\text{irradiation}}$	Ref
Cu-nanoparticle hydrogel	Cu-Nanoparticle	606 nm / 1.5 W cm ⁻²	12.5 °C/100 s	[1]
HA-DA/rGO	Reduced graphene oxide (rGO)	808 nm / 1 W cm ⁻²	~12.5 °C/100 s	[2]
CG/PDA@Ag	Polydopamine (PDA) nanoparticles	808 nm / 1 W cm ⁻²	~36 °C/100 s	[3]
CS/AM NSs	Antimonene nanosheets	808 nm /	~36 °C/100 s	[4]

hydrogel		1.5 W cm ⁻²		
PDA/Cu-CS	Polydopamine (PDA) & Cu nanosheets	808 nm / 1 W cm ⁻²	~36 °C/100 s	[5]
{Mo ₁₅₄ } hydrogel	Polyoxometalates: {Mo ₁₅₄ }	808 nm / 1 W cm ⁻²	~18 °C/100 s	[6]
CP@Au@DC-AC50	Gold nanorods (GNRs)	808 nm / 1 W cm ⁻²	~22 °C/100 s	[7]
PEDOT: PSS/agarose hydrogels	Poly(3,4-ethylenedioxythiophene): poly(styrene-sulfonate) (PEDOT:PSS)	808 nm / 1 W cm ⁻²	~24.5 °C/100 s	[8]
DOA-PVA	N-(2,4-Dihydroxybenzylidene)-4-aminophenol (DOA)	365 nm / 210 mW cm ⁻²	~52 °C/100 s	Our work

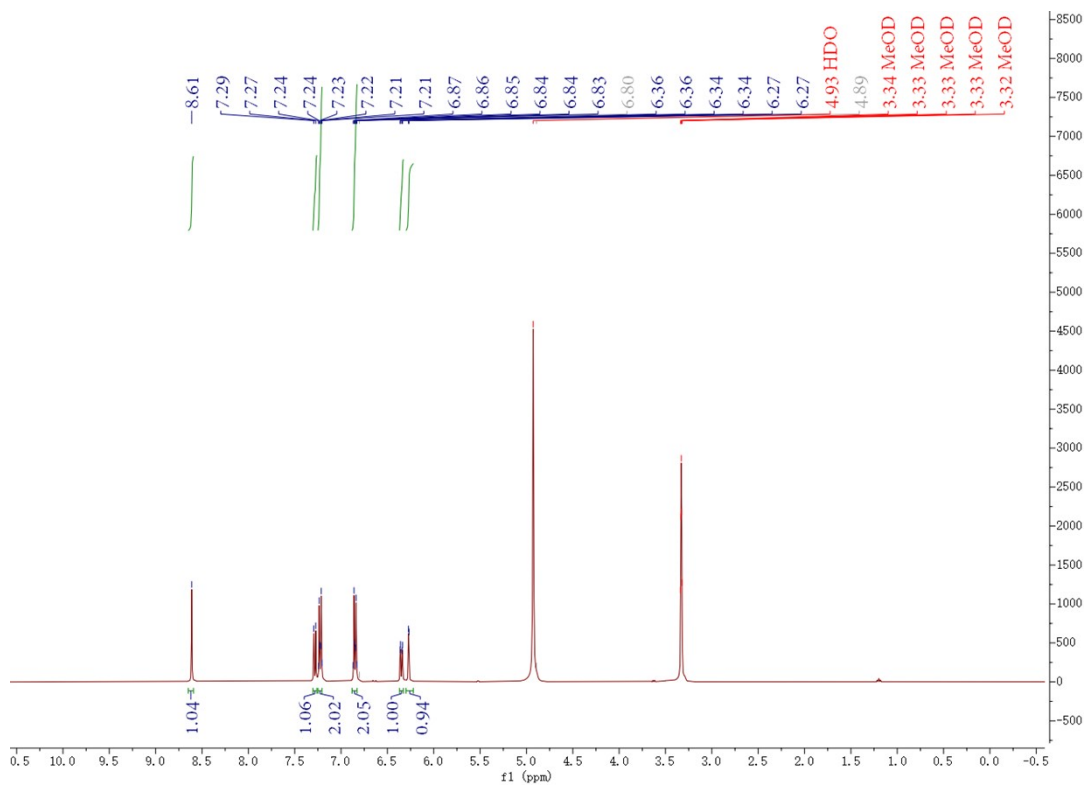


Figure S3. The ¹H NMR spectrum of DOA.

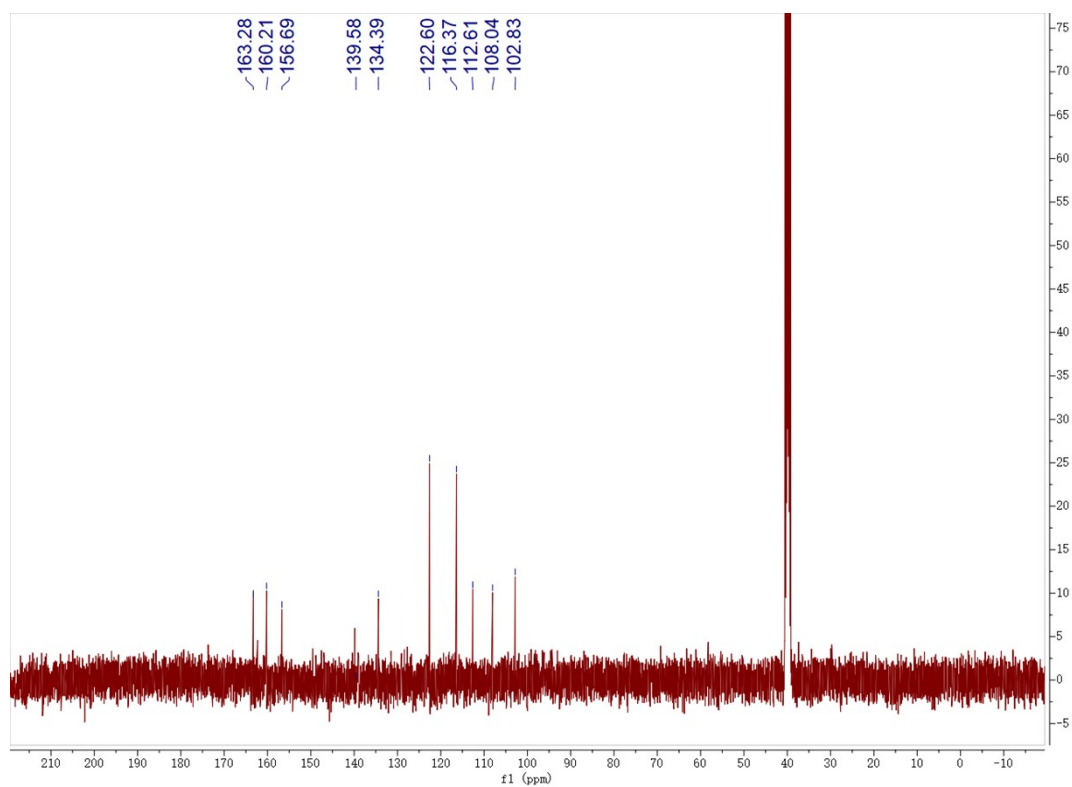


Figure S4. The ^{13}C NMR spectrum of DOA.

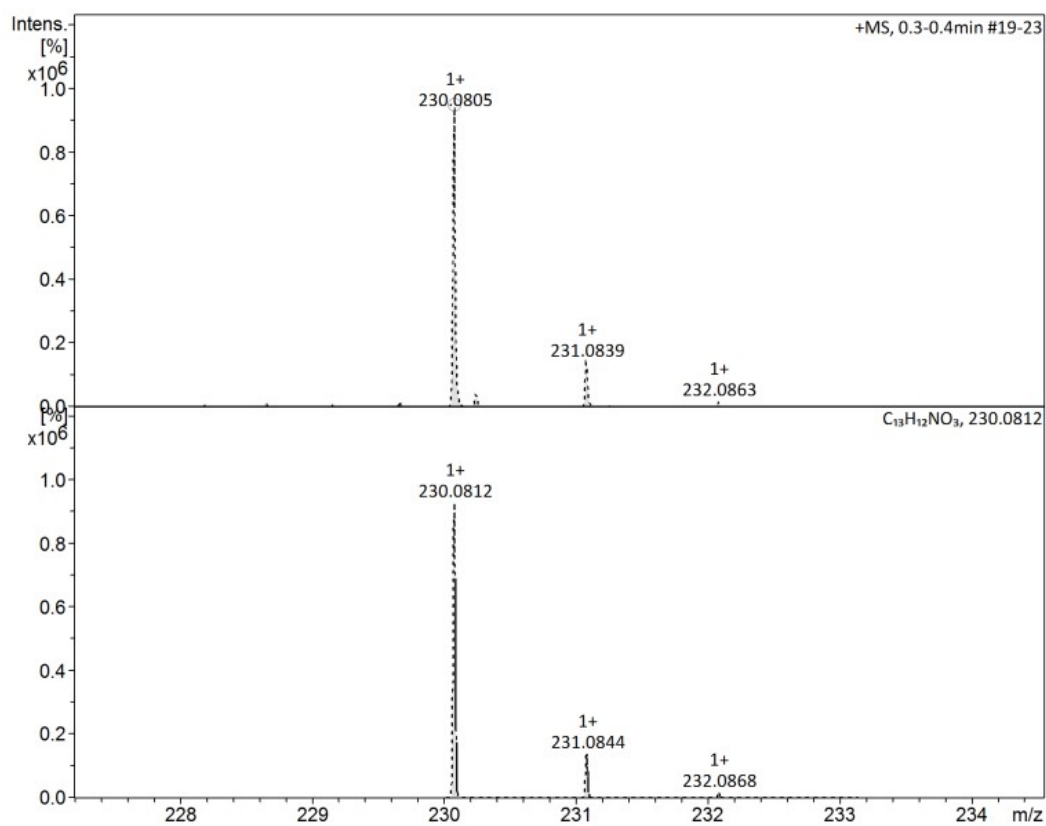


Figure S5. The HRMS spectrum of DOA.

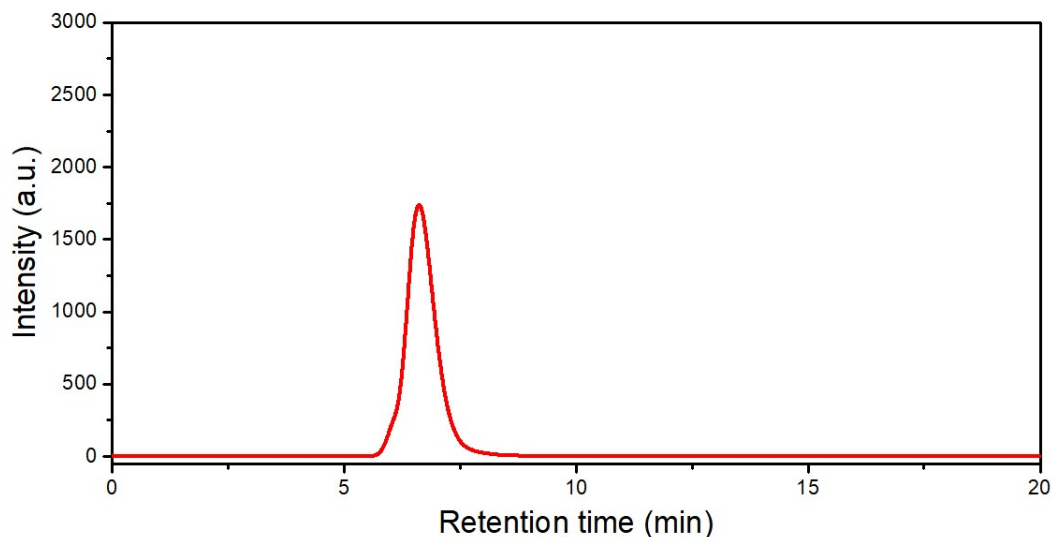


Figure S6. HPLC curve of DOA.

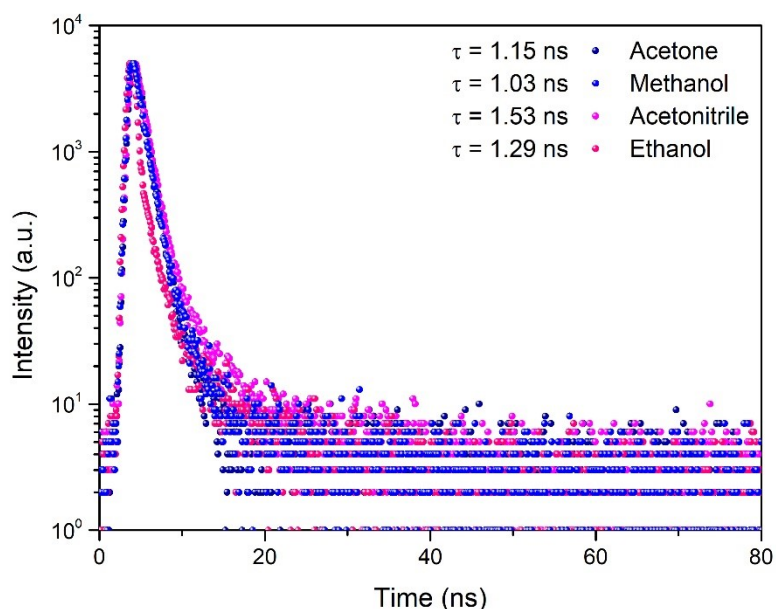


Figure S7. Fluorescence decay of DOA in different aprotic and protic solutions.

Table 3 The rate constants for both radiative and non-radiative decay in aprotic and protic solvents, as well as in PVA hydrogel.

	Ethanol ^a	Acetone ^a	Methanol ^a	Acetonitrile ^a	PVA ^b
	(*10 ⁷ s ⁻¹)				
k_r	1.14	1.49	1.15	3.71	1.28
k_{nr}	96.0	85.5	76.4	61.7	97.7

^a concentration: 2×10^{-5} mol L⁻¹, ^b Doping ratio: 1wt%

The rate constants of fluorescence can be obtained experimentally using equation:

$$k_r = \phi_f / \tau_f$$

$$k_{nr} = (1/\tau_f) - k_r$$

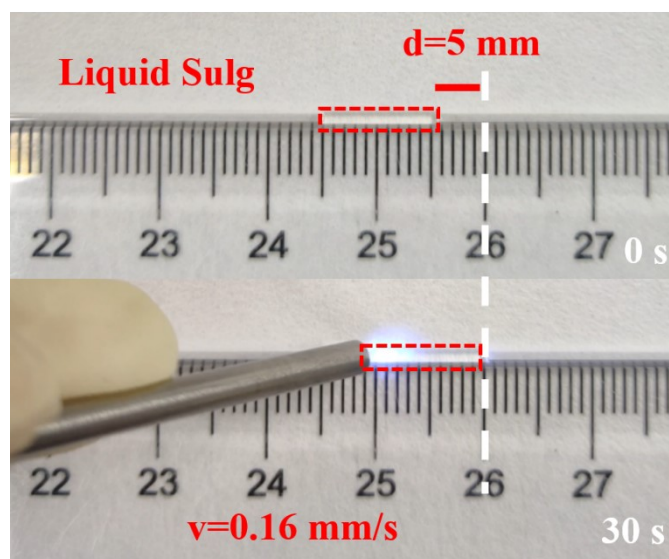


Figure S8. Light-induced motions of ethanol fluids of DOA (20 μ M) in glass capillaries. Note: Irradiating the liquid segment vertically from one end of the liquid plug (365 nm LED, 12 mW cm^{-2}), it can be observed to move forward.

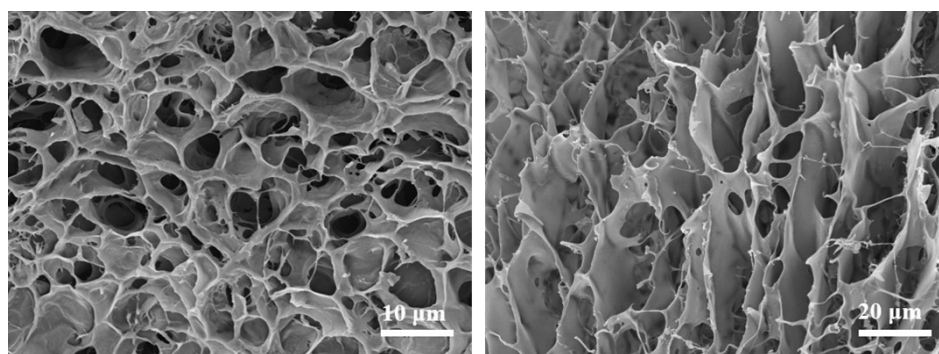


Figure S9. SEM images of DPVA hydrogel.

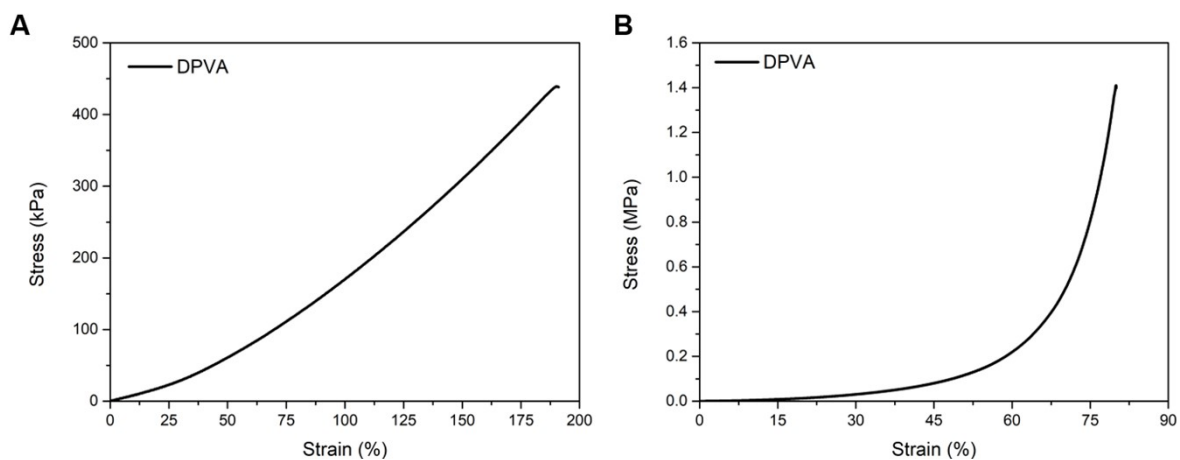


Figure S10. A) The tensile and B) compression stress-strain curve of DPVA hydrogel.

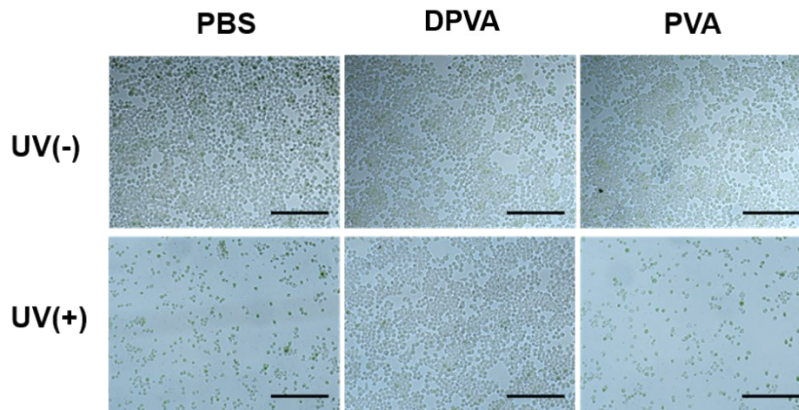


Figure S11. Micrograph of cytocompatibility evaluation by contacting with the L929 cells under different conditions.

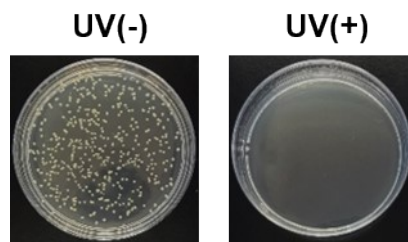


Figure S12. Pictures of the *S. aureus* treated by PBS with/without UV.

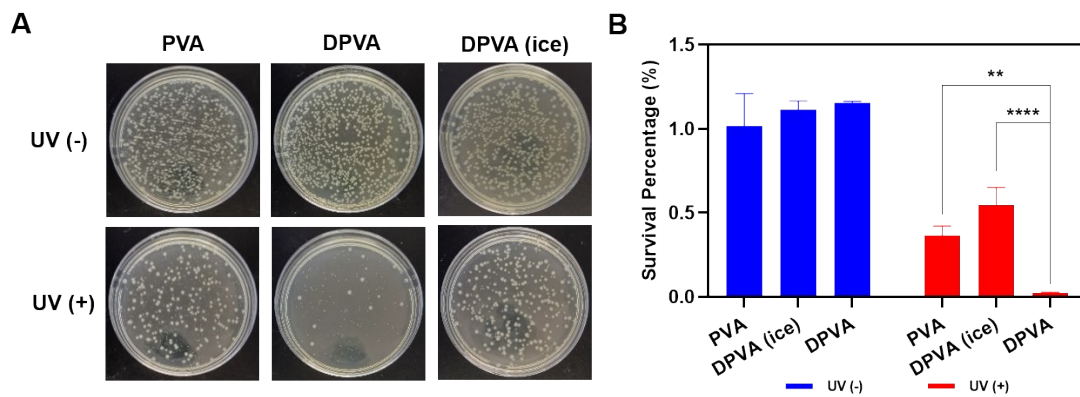


Figure S13. A) Pictures of *E. coli* grown on agar plates and B) corresponding inhibition percentage of *E. coli* with different treatments.

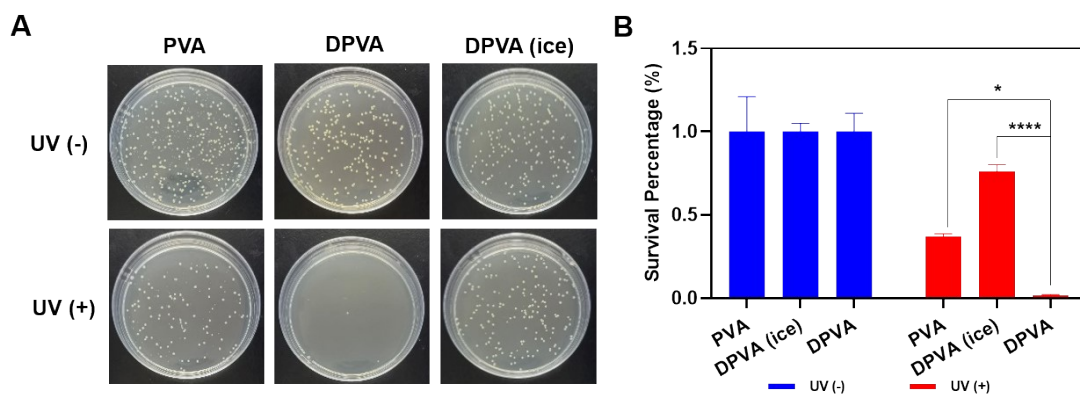


Figure S14. A) Pictures of *MRSA* grown on agar plates and B) the corresponding inhibition percentage of *MRSA*

with different treatments.

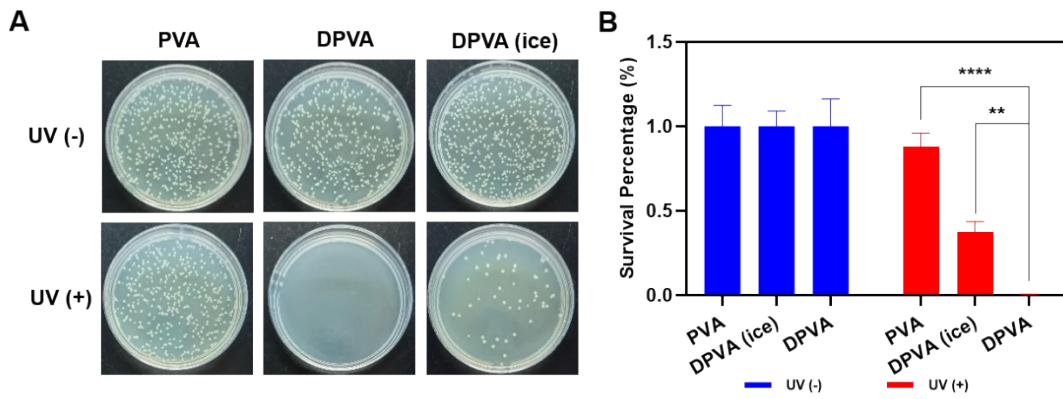


Figure S15. A) Pictures of *EIEC* grown on agar plates and B) the corresponding inhibition percentage of *EIEC* with different treatments.

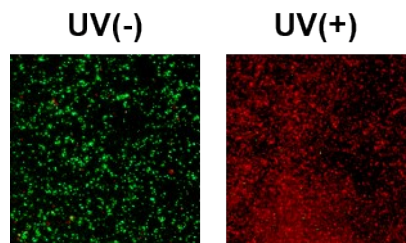


Figure S16. Confocal fluorescence photographs of *S. aureus* treated by PBS with/without UV.

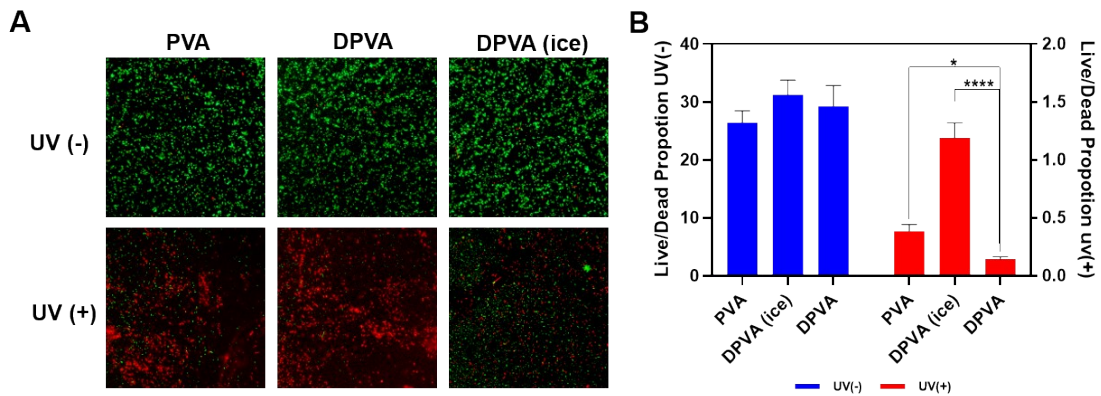


Figure S17. A) Confocal fluorescence photographs and B) the corresponding proportion of *E. coli* with different treatments.

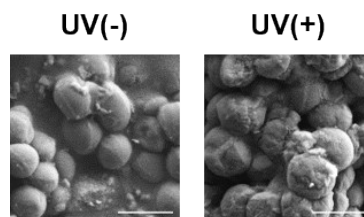


Figure S18. SEM photographs of *S. aureus* treated by PBS with/without UV (scale bar = 1 μ m).

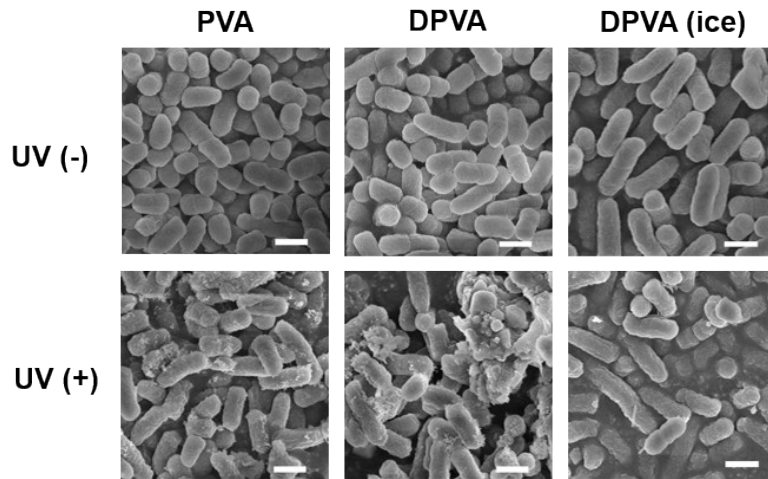


Figure S19. SEM photographs of *E. coli* after different treatments (scale bar = 1 μm).

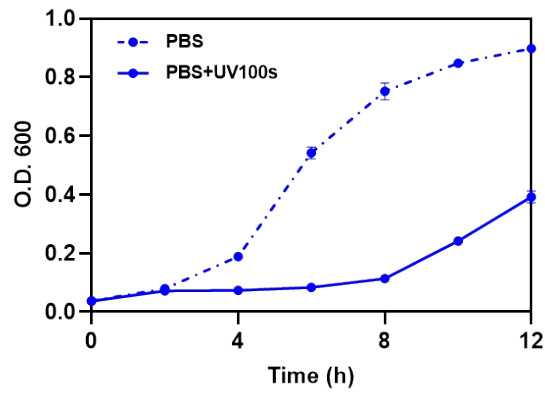


Figure S20. Growth curve of *S. aureus* treated by PBS with/without UV.

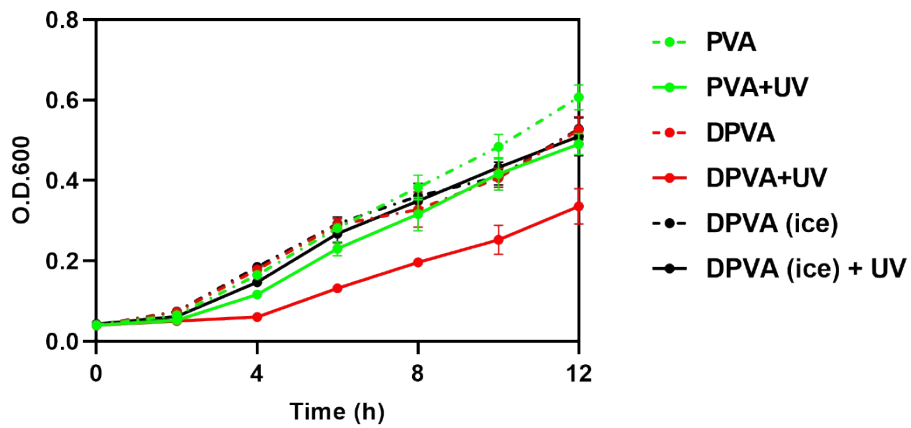


Figure S21. Growth curve of *E. coli* with different treatments.

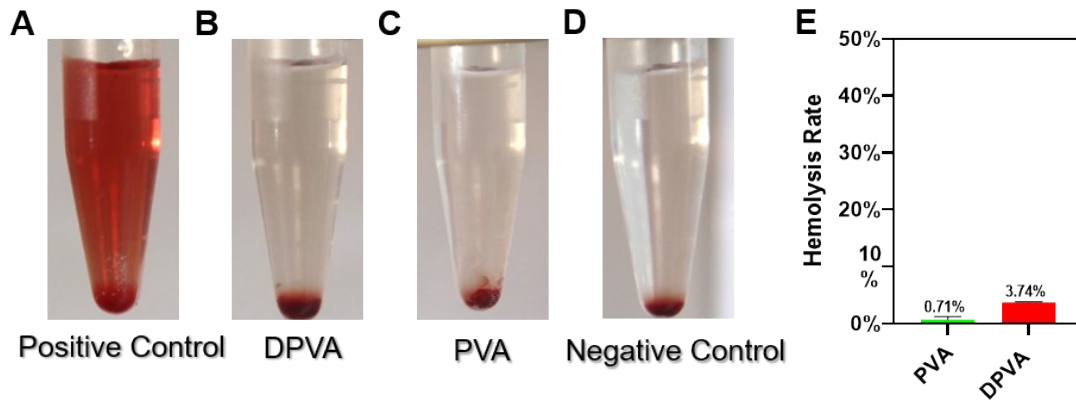


Figure S22. A) Pictures from hemolytic activity test of the hydrogels; B) Hemolytic percentage of the hydrogels.

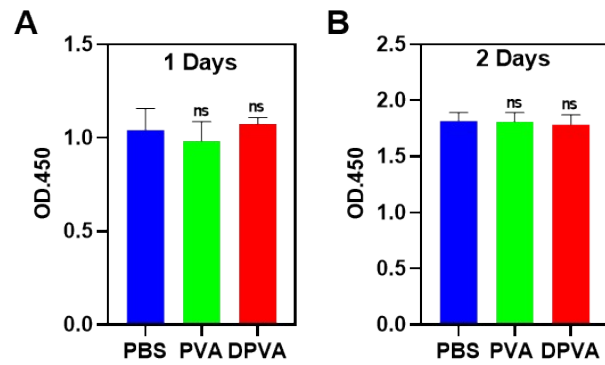


Figure S23. Cytopatibility evaluation of these hydrogels by contacting with the L929 cells.

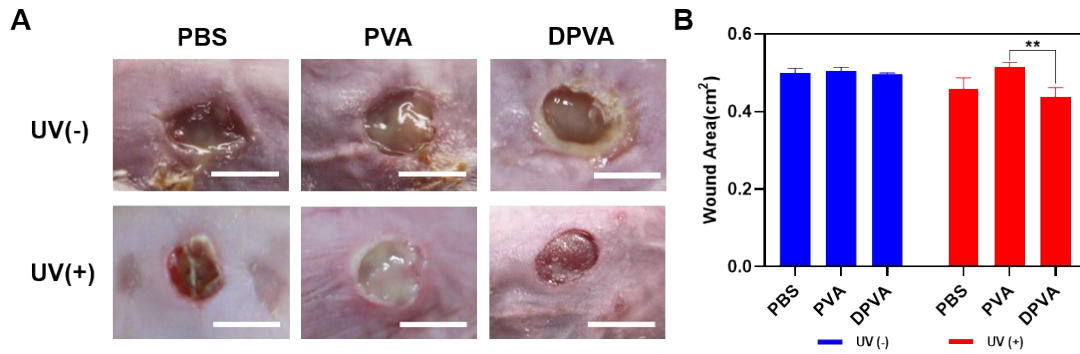


Figure S24. A) Photographs and B) wound area for each group of *MRSA*-infected wounds with different treatments on Day 7 (scale bar = 1 cm).

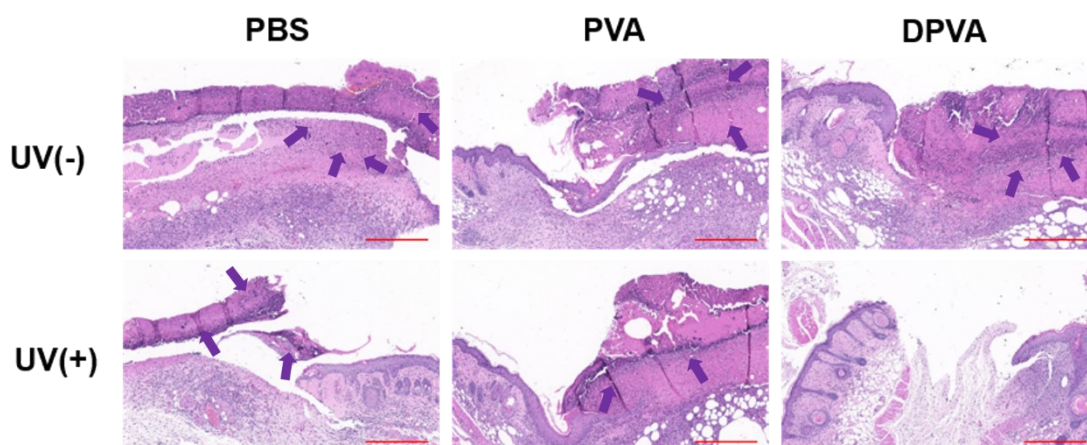


Figure S25. H&E staining of the skin tissues from the wound edges for each group of *MRSA*-infected wounds with different treatment on Day 7 (the purple arrows: area of inflammation) (scale bar = 500 μm).

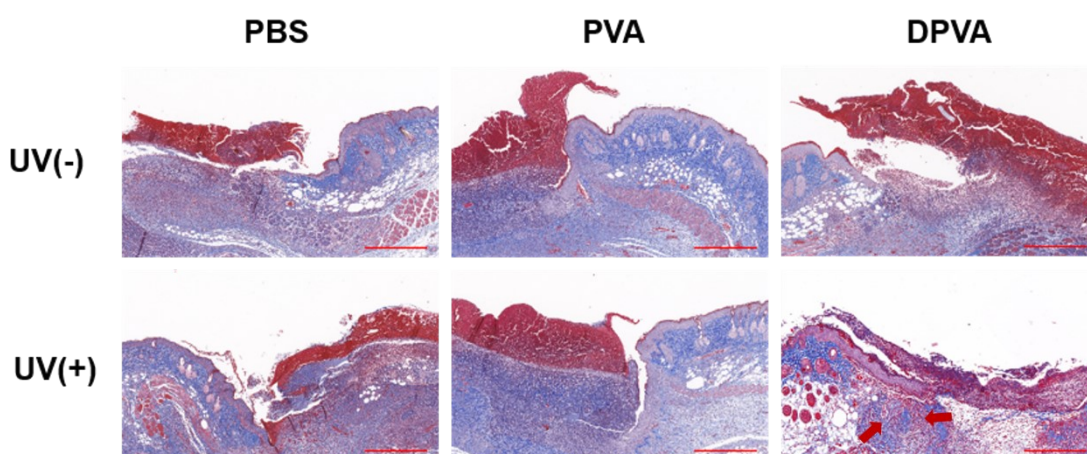


Figure S26 Masson's trichrome staining of the skin tissues from the wound edges for each group of *MRSA*-infected wounds with different treatment on Day 7 (the red arrow: collagen fibers) (scale bar = 500 μm).

References

1. S. Chen, F. Tang, L. Tang and L. Li, *ACS Applied Materials & Interfaces*, 2017, **9**, 20895-20903.
2. Y. Liang, X. Zhao, T. Hu, B. Chen, Z. Yin, P. X. Ma and B. Guo, *Small*, 2019, **15**, 1900046.
3. X. Qi, Y. Huang, S. You, Y. Xiang, E. Cai, R. Mao, W. Pan, X. Tong, W. Dong, F. Ye and J. Shen, *Advanced Science*, 2022, **9**, 2106015.
4. X. Zhao, Y. Liang, Y. Huang, J. He, Y. Han and B. Guo, *Advanced Functional Materials*, 2020, **30**, 1910748.
5. Q. Xu, M. Chang, Y. Zhang, E. Wang, M. Xing, L. Gao, Z. Huan, F. Guo and J. Chang, *ACS Applied Materials & Interfaces*, 2020, **12**, 31255-31269.
6. G. Guedes, S. Wang, F. Fontana, P. Figueiredo, J. Lindén, A. Correia, R. J. B. Pinto, S. Hietala, F. L. Sousa and H. A. Santos, *Advanced Materials*, 2021, **33**, 2007761.
7. S. Wang, B. Chen, L. Ouyang, D. Wang, J. Tan, Y. Qiao, S. Ge, J. Ruan, A. Zhuang, X. Liu and R. Jia, *Advanced Science*, 2021, **8**, 2004721.
8. Y. Ko, J. Kim, H. Y. Jeong, G. Kwon, D. Kim, M. Ku, J. Yang, Y. Yamauchi, H.-Y. Kim, C. Lee and J. You, *Carbohydrate Polymers*, 2019, **203**, 26-34.